

Anlotinib inhibits the proliferation and induces apoptosis by inactivating the AKT pathway in androgen receptor-negative prostate cancer cells

Yan XU¹, Ji ZHENG², Zhi-Ying YE^{3,*}

¹Department of Geriatrics, Hwa Mei Hospital, Ningbo No. 2 Hospital, University of Chinese Academy of Sciences, Ningbo, China; ²Department of Radiology, Hwa Mei Hospital, Ningbo No. 2 Hospital, University of Chinese Academy of Sciences, Ningbo, China; ³Department of Medical Imaging, Hwa Mei Hospital, Ningbo No. 2 Hospital, University of Chinese Academy of Sciences, Ningbo, China

*Correspondence: 65435946@qq.com

Received June 24, 2022 / Accepted August 16, 2022

Prostate cancer is one of the most frequently diagnosed cancers in men. The medical treatment of metastatic prostate cancer relies heavily on androgen deprivation. The present study aimed to explore the inhibitory effect of anlotinib on androgen receptor (AR)-negative prostate cancer cell lines *in vitro* and investigate its mechanism of action. Two prostate cancer cell lines, DU145 and PC-3, were treated with different concentrations (0–80 μ M) of anlotinib. Cell proliferation was accessed by CCK-8 assay and EdU staining. Cell nuclear morphology was observed after DAPI staining, cell apoptosis level was evaluated by Annexin-V-FITC/PI staining, and western blot was used to detect the proliferation- and apoptosis-related proteins. The potential interaction between anlotinib and AKT was revealed by molecular docking. After treatment with anlotinib, the cell proliferation rate was significantly inhibited in a dose-dependent manner. The DAPI staining showed that anlotinib could induce apoptosis. Further, Annexin V/PI double staining confirmed the occurrence of apoptosis, accompanied by the increase of cleaved caspase-3 and activated PARP. Moreover, anlotinib significantly decreased the phosphorylation of protein kinase B (AKT) and its downstream pathway proteins in prostate cells ($p < 0.05$). Experiments further confirmed that the activation of the AKT pathway reversed the inhibitory effect of anlotinib on DU145 and PC-3 cell proliferation. In addition, molecular docking analysis revealed potential interactions between anlotinib and AKT1 at multiple sites. Overall, the present study suggested that anlotinib could inhibit the proliferation and induce apoptosis in the AR-negative prostate cancer cell lines, possibly via the inactivation of the AKT pathway.

Key words: anlotinib, protein kinase B pathway, prostate cancer, apoptosis, proliferation

Prostate cancer is the most frequent malignant tumor in Europe and America [1]. The differences in the incidence of prostate cancer in different races are pretty evident. The incidence of prostate cancer in China is lower than in Europe and the United States. However, in recent years, the number of prostate cancer patients in China has gradually increased [1, 2]. Prostate cancer has almost no symptoms, and it is often in the advanced stage when it is discovered. Through regular physical examinations and blood tests, the determination of prostate-specific antigen tumor markers to promote early detection and early diagnosis is the only effective way to reduce their mortality. Patients with prostate tumors beyond stage B2, where cancer has already invaded the prostate tissue or metastasized, are often unable to undergo radical surgery. Therefore, they may rely only on endocrine therapy [3]. Endocrine therapy is the most essential and effective palliative therapy. However, in most patients, the tumor is

commonly converted to hormone-independent prostate cancer. Once converted, patients are no longer sensitive to endocrine therapy. Although chemotherapy is the first-choice treatment for androgen receptor (AR)-negative prostate cancer, it may also lead to drug resistance and several serious adverse effects, leading to a poor prognosis for patients [4]. Therefore, the development of drugs for AR-negative prostate cancer is urgently needed.

In addition to the traditional androgen deprivation drugs, other regimens such as abiraterone targeted drugs have also been recently used for prostate cancer treatment [5], such as enzalutamide [6], olaparib [7, 8], bevacizumab, tasquinimod, and cabozantinib [9–11]. There are many drugs under development, for example, the phosphoinositide 3-kinase (PI3K)-mammalian target of rapamycin (mTOR) inhibitor BEZ235 [12], protein kinase B (AKT) inhibitor GDC0068 [13], and the endothelin receptor antagonist atrasentan [14].

To date, most of these drugs are still under clinical research. Therefore, currently, the available targeted drugs for prostate cancer treatment are limited.

Anlotinib is a new multi-target tyrosine kinase inhibitor and can effectively inhibit vascular endothelial growth factor (VEGFR), platelet-derived growth factor receptor, and other kinases [15], and exerts anti-tumor and anti-angiogenic properties [16]. The main clinical application of anlotinib is non-small cell lung cancer [17]. Furthermore, the effect of anlotinib on different solid tumors, including small cell lung cancer, uterine cancer, colorectal cancer, and esophageal squamous cell carcinoma, has been investigated in several clinical trials [17, 18]. Among them, most studies show that the anticancer effect of anlotinib is related to the Akt pathway. A recent clinical study has shown that anlotinib has a therapeutic effect on prostate cancer, but the specific mechanism remains to be confirmed [19]. Therefore, this study will explore the inhibitory effect of anlotinib on the prostate and provide an experimental basis for clinical application.

Materials and methods

Cell culture. The human prostate cancer cell lines DU145 and PC-3 were from Zhejiang Ruyao Biotechnology. DU145 cells were cultured in 90% MEM (GIBCO, 41500034) and 10% FBS, and PC-3 cells were cultured in 90% F-12 (GIBCO, 21700075) and 10% FBS, in a constant temperature incubator at 37°C and 5% CO₂. Every 2–3 days, the supernatant was removed, and the cells were trypsinized following the centrifugation. The experiment was performed until cells reached the logarithmic growth phase.

Cell proliferation assay. For cell counting kit-8 (CCK-8) assay, DU145 and PC-3 cells were collected and adjusted the concentration of the cell suspension to 5×10⁴ cells/ml. Subsequently, a total of 100 µl/well of the cell suspension were seeded into 96-well plates and incubated at 37°C in 5% CO₂ overnight. Each well was then supplemented with 100 µl of diluted anlotinib (purchased from Selleck Corporation (Houston, TX, USA)) at different concentrations (80, 40, 20, 10, 5, 2.5, and 1.25 µM), and incubated the plates at 37°C in 5% CO₂. Cells were harvested at 24, 36, and 48 h following anlotinib addition. 20 µl of CCK-8 reagent was added to each well, and the cells were incubated for another 4 h at 37°C. The OD value was recorded by the microplate reader (Multi-skan GO, Thermo Fisher, USA) at 450 nm, where untreated cells served as the blank control group. Calculated the cell proliferation inhibition rate (%) as follows: (1 – experimental group OD value/control group OD value) × 100%.

EdU assay. Treated the prostate cancer cells with 10 µM anlotinib, the treated cells from each group were prepared into single-cell suspension and adjusted the cell concentration to 1×10⁷/ml, then the EdU proliferation detection kit (Cat No: C0081L, Beyotime Biotechnology Co., Ltd.) was used. Briefly, a pre-warmed EdU working solution was added to the cells (37°C, final concentration of 10 µM), and then incubation

was continued for 2 h at 37°C. After the completion of EdU-labeled cells, the culture medium was removed, 1 ml of fixative solution was added, the cells were washed three times with 1 ml of washing solution, and 1 ml of permeabilizing solution was incubated at room temperature for 10–15 min. Finally, the reaction solution was added and incubated for 30 min at room temperature in the dark. After the reaction solution was washed off, results were observed and counted with a fluorescence microscope (Leica, DM2500).

DAPI staining. DU145 and PC-3 cells treated with 0, 2.5, 5, and 10 µM of anlotinib for 48 h were grown on glass coverslips. The slides were immersed in pre-cooled methanol and fixed. Subsequently, cells were treated with 1 µg/ml DAPI staining solution and incubated at room temperature for 1–2 min. The excess solution was absorbed with filter paper. Finally, the glass slides were observed under a fluorescence microscope at 360–400 nm wavelength to identify the changes in the nucleus morphology.

Cell cycle analysis. Propidium iodide (PI) staining and flow cytometry (Attune NXT, ABI) were used to detect the cell cycle. Cells were seeded on 6-well plates at a density of 5×10⁵ cells/well. The cells were incubated with different concentrations of anlotinib (0, 2.5, 5, and 10 µM) in a humid environment containing 5% CO₂ for 24 h at 37°C. Then, the cells (1×10⁶) were collected, washed twice with PBS, and fixed overnight with cold ethanol (70%) at 4°C. A PI solution (0.02% Triton X-100 and 50 mg/ml RNase) was used for cell staining in the dark for approximately 30 min. Flow cytometry was used to detect 2×10⁵ cells with a standard procedure. FlowJo software (FlowJo™ v10.7) was used to analyze the data.

Apoptosis evaluation by Annexin V-FITC/PI staining. The apoptosis rate of cells was determined with an Annexin V-FITC/PI double staining kit (BD Biosciences). Following treatment of cells with 0, 2.5, 5, and 10 µM anlotinib for 24 h, the cell suspension was centrifuged at 600 g/min, and cells were resuspended in the buffer after discarding the supernatant. Subsequently, 5 µl of Annexin V and 5 µl of PI were added to the cell suspension and incubated at room temperature for 15 min in the dark. The Attune NxT flow cytometer (Life Technologies; Thermo Fisher Scientific Inc.) was used to determine prostate cell apoptosis. Each experiment was repeated three times independently.

Western blotting. Prostate cells were harvested by centrifugation following treatment with 0, 2.5, 5, and 10 µM anlotinib for 48 h. The RIPA buffer (Solarbio, China) was added to cells, incubated on ice for 10 min to lyse cells, and centrifuged at 12 000×g, 4°C for 15 min. The BCA protein assay kit (P0011, Byotime, China) was used to quantify protein concentration. Subsequently, total proteins were separated by 10% SDS-PAGE, transferred to the polyvinylidene fluoride membrane at 250 mA, and blocked with 5% skim milk at room temperature for 1 h. Then the following primary antibodies were added: Bax (CST, #5023), Bcl-2 (CST, #3498), cleaved caspase-3 (CST, #9664), caspase-3 (CST, #9662), cleaved PARP (CST, #5625), PARP (CST,

#9532), β -Actin (CST, #3700), phospho-PI3 kinase p85 (CST, #4228), PI3 Kinase p85 (CST, #4257), phospho-Akt (CST, #4060), Akt (CST, #9272), PCNA (CST, #13110), and incubated at 4°C overnight. The next day, the membranes were washed with TBST (containing 0.15% Tween 20) three times, then incubated with a horseradish peroxidase-labeled secondary antibody at room temperature for 2 h. Finally, the membranes were washed three times and the immune reactive bands were visualized using an ECL kit and a protein imager. β -actin served as the internal reference protein for relative protein quantification. ImageJ software was used to quantify the bands.

Cell invasion assay. The invasion ability of DU145 and PC-3 cells was determined with a Transwell assay. Matrigel was diluted with the medium at 1:8 and used to coat the upper chamber, then incubated at 37°C for 30 min to make the Matrigel polymerized, and hydrated the basement membrane before use. 1×10^4 cells were resuspended in 200 μ l DMEM containing different concentrations of anlotinib and inoculated into the 24-well plates. The lower chamber was supplemented with 0.5 ml of DMEM containing 10% FBS to induce cell migration. Following incubation for 24 h, the cells on the surface of the Transwell membranes were fixed with 4% paraformaldehyde, stained with crystal violet, and observed with a microscope (at 200 \times magnification). The number of the invaded cells was calculated in five randomly selected fields from each field.

Molecular docking. The 3D structure of anlotinib was downloaded from the PubChem database (<https://pubchem.ncbi.nlm.nih.gov/>). Its structure was optimized in the MMFF94 force field using the OpenBabel 2.4.1 software. Furthermore, the 3D structure was downloaded from the RCSB Protein Data Bank (<http://www.rcsb.org/>) in order to obtain the protein used for the docking of this subject. The AutodockTools 1.5.6 software was applied to search and define the rotatable bonds of the compound. We removed the water, added hydrogen atoms and charges, and the project was then saved in PDBQT format. Molecular docking analysis was performed using the Autodock vina 1.1.2 software. The coordinates of protein active sites were determined based on the position of protein ligands, while for other parameters, the default values were used. Finally, the conformation with the lowest docking binding energy was selected for analysis. And the Discovery Studio 2017 software was used to show the interaction between molecules.

AKT kinase activity The cells from different treatment groups were washed with pre-cooled PBS, 1 ml cell lysis buffer was added, and incubated in ice for 10 min. The AKT activator SC79 (cat. no. SF2730) was from Beyotime Institute of Biotechnology (Shanghai, China) and the AKT kinase activity assay kit was from Abcam (ab139436). The experiments were performed according to the instructions to operate.

Statistical analysis. All statistical analyses were performed using the SPSS 20.0 statistical software. All data are expressed

as $\bar{x} \pm$ standard deviation (SD). Comparisons among multiple groups were carried out using one-way analysis of variance (ANOVA) and two groups were compared with a t-test. A p-value <0.05 was considered to indicate a statistically significant difference. The GraphPad Prism 8.0 software was used to visualize the statistical analyses.

Results

The inhibitory effect of anlotinib on the proliferation of different prostate cancer cells. After treatment with different concentrations of anlotinib (Figure 1A) for 48 and 72 h, the proliferation of PC-3 cells was significantly reduced and showed a dose-dependent manner (Figure 1B). The IC₅₀ values of DU145 cells at 48 h and 72 h (Figures 1B, 1C) were 8.78 and 7.11 μ M, respectively, while those of PC-3 cells were 6.04 μ M and 4.31 μ M, respectively. These findings revealed that anlotinib inhibited prostate cancer cell proliferation in a dose- and time-dependent manner. Furthermore, after the addition of 10 μ M anlotinib, the EdU cell proliferation assay was performed by fluorescence microscopy (Figures 1D, 1E), which showed that the number of EdU positive prostate cancer cells was decreased significantly (from 57–64% to 37–45%) when compared with the control group (Figure 1E, p<0.05). Furthermore, the inhibitory effect of anlotinib on PC-3 cells' proliferation was more efficient than that on DU145 cells.

The effect of anlotinib on the growth and invasion of prostate cancer cells. Subsequently, flow cytometry was carried out to evaluate cell cycle progression of control and anlotinib-treated prostate cancer cells treated with different concentrations of anlotinib. Increasing concentrations of anlotinib significantly increased the percentage of cells in the G2/M phase (Figures 2A, 2B), the control of PC-3 was 14.03% and the 10 μ M treated group was 35.26%. Similarly, in DU145 cells, the control group was 12.25%, 10 μ M treated group was 45.69%. This indicates that anlotinib arrested the cell cycle at the G2/M phase in prostate cancer cells. The Transwell assay results showed that anlotinib effectively inhibited PC-3 and DU145 cells invasion (Figure 2C). This result showed that anlotinib could significantly inhibit the invasion of prostate cancer cells (p<0.05), and the inhibitory effect was more significant when PC-3 and DU145 cells were treated with 5 μ M and 10 μ M anlotinib (p<0.01). The above results suggest that anlotinib can arrest the cycle of prostate cancer cells and attenuate the invasive ability of prostate cancer cells.

The effect of anlotinib on cell apoptosis. After DAPI staining it could be observed that the number of cells decreased after being treated with anlotinib. This effect was more evident with increasing concentrations of anlotinib (Figure 3A). In addition, cell apoptosis was determined by flow cytometry. Anlotinib significantly induced apoptosis, and the apoptosis rate was elevated with increasing concentrations of anlotinib. The cell apoptosis rate of PC-3 cells was

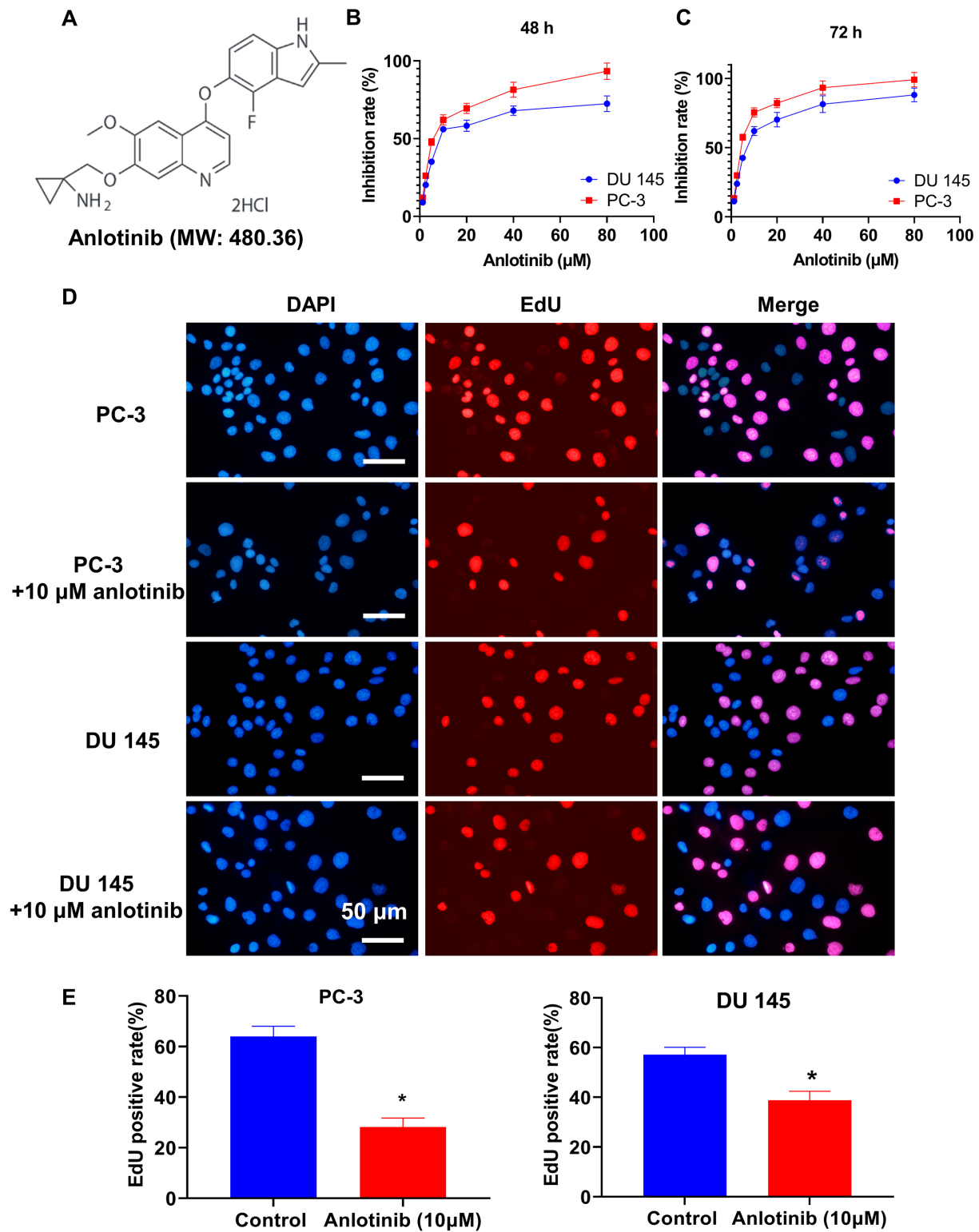


Figure 1. Effect of different concentrations of anlotinib on prostate cancer cell proliferation at 48 h and 72 h. A) Molecular structure of anlotinib. Following incubation with anlotinib for 48 h B) and 72 h. C) The cell viability and the IC_{50} . D) EdU cell proliferation was detected by fluorescence microscopy, scale bar = 50 μ M. E) Statistical quantification diagram of positive results of EdU cell proliferation test. Compared with the control group, * $p < 0.05$

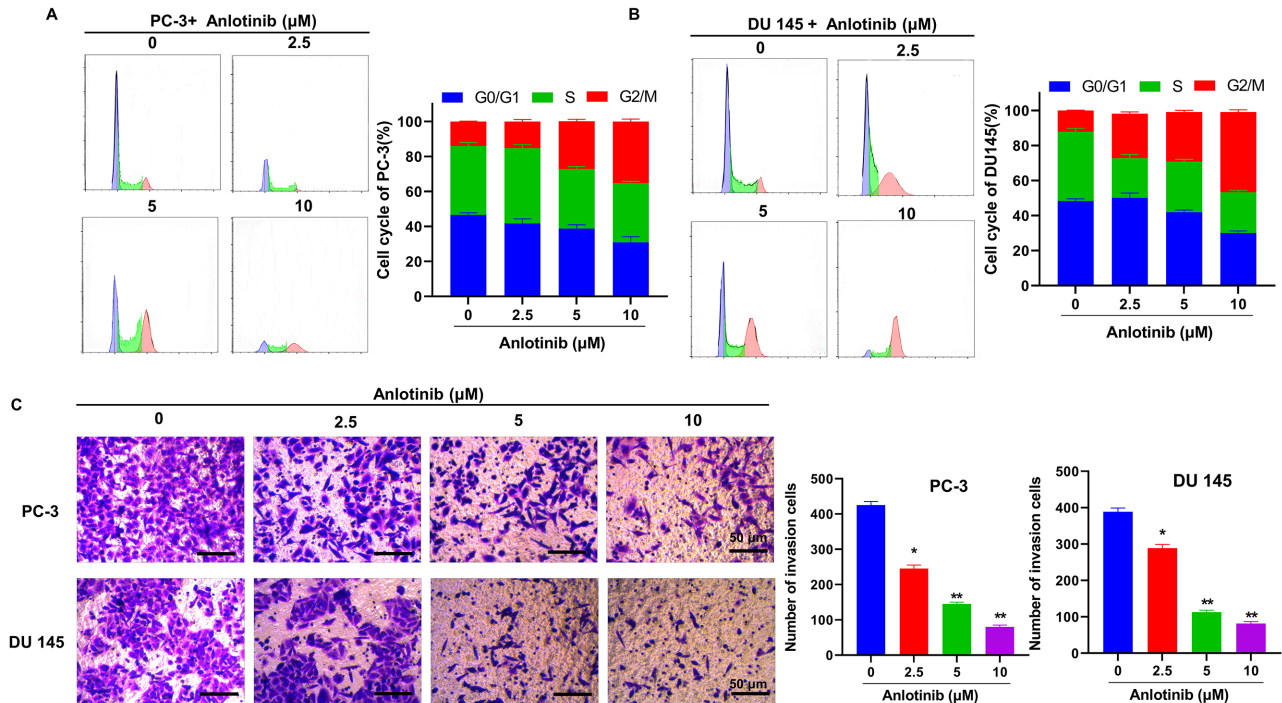


Figure 2. The effect of anlotinib on the growth and proliferation of PC-3 and DU145 cells. A) Graph showing the nuclear fluorescence after DAPI staining, scale bar = 50 μM. B) Cell cycle distribution was assessed by flow cytometry. C) Statistical analysis of the flow cytometry results using the Flow Jo software. D) Transwell experiment results are shown. E) A statistical quantification chart of the number of invaded cells. * $p < 0.05$, compared with the blank control group (0 μM), ** $p < 0.01$, compared with the blank control group (0 μM)

from 5.04% (0 μM) to 23.68% (10 μM) (Figure 3B, $p < 0.01$), and apoptosis rate of DU145 cells was from 5.78% (0 μM) to 18.37% (10 μM) ($p < 0.01$). Furthermore, the expression levels of the apoptosis-associated proteins were detected by western blot analysis (Figure 3C). Among the above proteins, the expressions of the cleaved forms of caspase-3 and PARP were significantly upregulated following treatment with anlotinib in a dose-dependent manner (Figure 3D, $p < 0.05$). The apoptotic protein Bax increased significantly and the anti-apoptotic protein Bcl-2 decreased significantly ($p < 0.05$). These findings indicated that anlotinib could induce apoptosis in PC-3 and DU145 prostate cancer cells.

Anlotinib inhibits the growth of prostate cancer cells via the AKT pathway. The phosphorylation status of the AKT pathway-associated proteins was investigated by western blot. The result revealed that the phosphorylation levels of PI3K and AKT in PC-3 and DU145 cells were downregulated with increasing concentrations of anlotinib (Figures 4A, 4B). Subsequently, recovery experiments were carried out to determine whether anlotinib was involved in the AKT signaling pathway. Therefore, PC-3 and DU145 cells were co-treated with 4 μg/ml of the AKT activator SC79 and 10 μM anlotinib. The co-treatment of PC-3 and DU145 cells recovered the activity of AKT and its downstream molecules (Figures 4C, 4D), while no significant differences

were observed between the control and co-administration groups. However, when cells were co-treated with SC79, the phosphorylation of AKT and its downstream molecules was restored. Furthermore, the effect of SC79 on cell viability was also evaluated (Figure 4E). In addition, after detecting the apoptosis-related protein, including cleaved caspase-3, and PARP. The western blot results showed that the apoptosis-related protein cleaved caspase-3 and PARP, Bax in prostate cancer cells were significantly activated after anlotinib treatment (compared with the control group, $p < 0.05$), and Bcl-2 decreased significantly ($p < 0.05$). The addition of SC79 effectively inhibited the activation of apoptotic proteins induced by anlotinib (Figures 4F, 4G). Therefore, co-treatment with SC79 reversed the anti-proliferative effects of anlotinib on prostate cancer cells ($p < 0.05$). Furthermore, molecular docking was analyzed between anlotinib and the AKT1 (Figure 4H). The affinity score of AKT1 was $-7.9 \text{ kcal/mol}^{-1}$. The analysis identified van der Waals interactions between the compound and the amino acid residues LEU158, VAL166, LYS277, ASN280, MET282, ASP293, PHE439, and PHE443, hydrophobic interactions with the amino acid residues PHE163, PHE238, and PHE29, electrostatic interactions with the amino acid residues GLU236, GLU279, and ASP440, and formation of hydrogen and halogen bonds with the amino acid residues

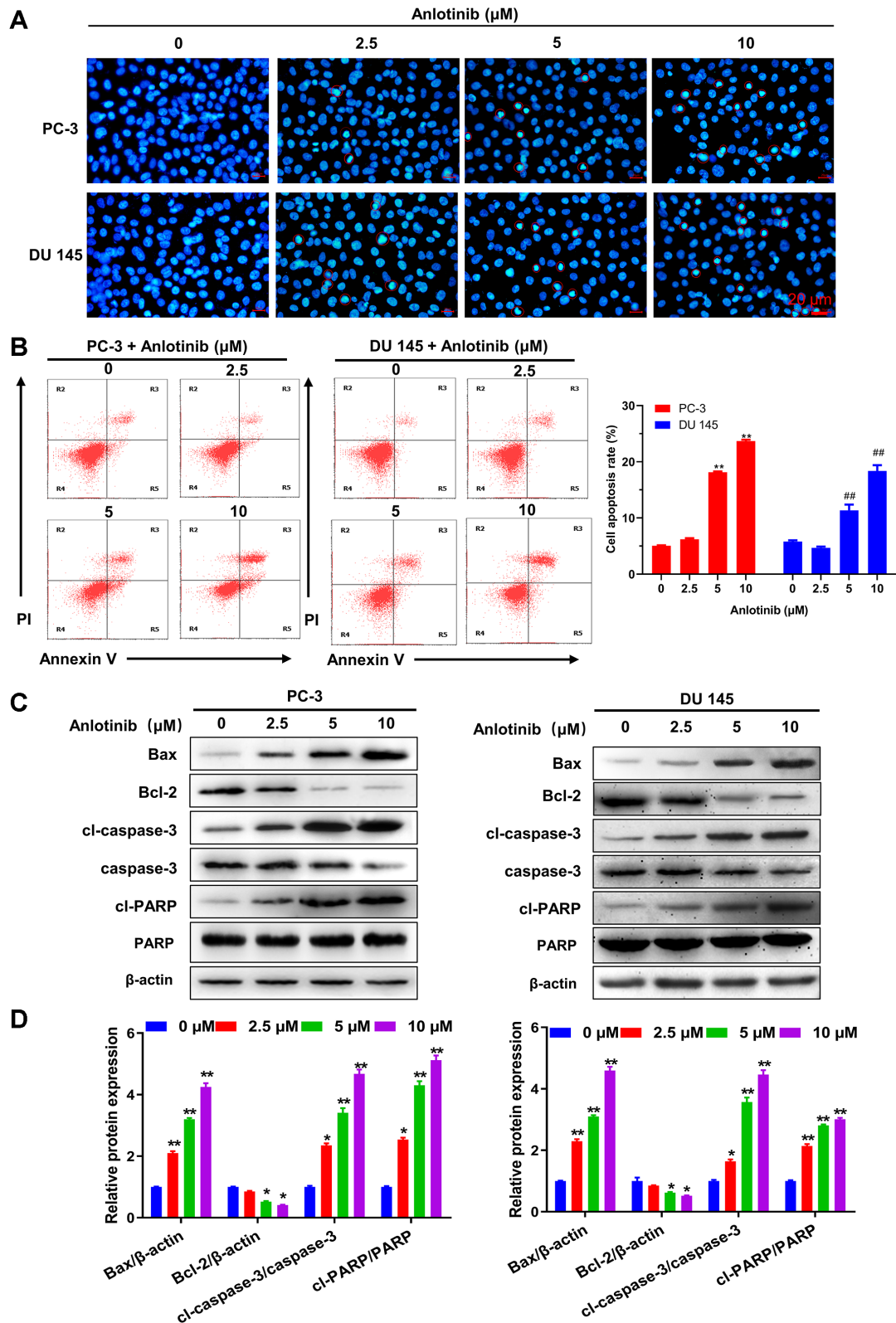


Figure 3. Analysis of the effect of different concentrations of anlotinib on PC-3 and DU145 cells apoptosis by flow cytometry. A) The Annexin-V FITC/PI double staining method was used to detect PC-3 and DU145 cells' apoptosis. B) Quantification of PC-3 and DU145 cells' apoptosis rate. C) Western blot analysis of apoptosis-related proteins. D) Quantification of protein expression. * $p < 0.05$, ** $p < 0.01$, compared with the blank control group (0 μM)

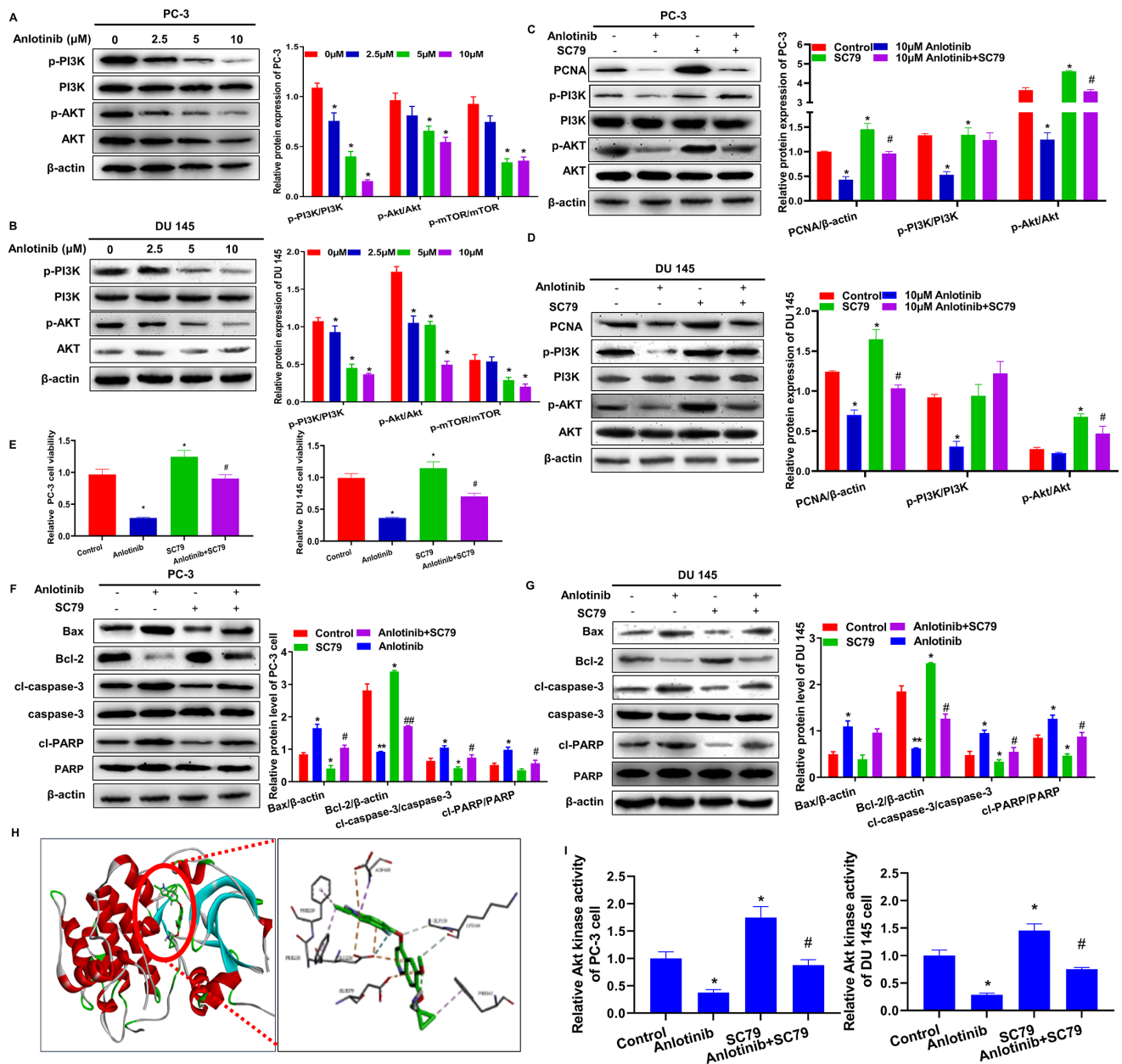


Figure 4. Anlotinib inhibited the proliferation of PC-3 and DU145 cells via regulating the AKT pathway. **A)** Western blot analysis of the phosphorylation of AKT pathway-related proteins. **B)** Quantification of protein expression. * $p < 0.05$, compared with the 0 μM anlotinib group. **C)** The effect of AKT activator on the phosphorylation of AKT pathway- and cancer cell proliferation-associated proteins. **D)** Quantification of protein expression, * $p < 0.05$, compared with the 0 μM anlotinib group. # $p < 0.05$, compared with 10 μM anlotinib group. **E)** Cell viability was evaluated following co-treatment of cells with the SC79. * $p < 0.05$, compared with the control group. # $p < 0.05$, compared with anlotinib group. **F)** Western blotting results of apoptotic proteins; **G)** Quantitative statistical chart of western blotting results, * $p < 0.05$, compared with the blank control group (0 μM). # $p < 0.05$, compared with anlotinib group. **H)** Molecular docking results of anlotinib and Akt1 protein interaction. **I)** Test results of Akt kinase activity. * $p < 0.05$, compared with the control group (0 μM). # $p < 0.05$, compared with the anlotinib group

LYS160 and GLU236. These interactions indicated that the docking was relatively stable. The Akt kinase activity test showed that anlotinib could inhibit the Akt kinase activity of prostate cancer cells, and there was a significant difference compared with the normal control group. The

addition of SC79 could reverse the effect of anlotinib on Akt kinase activity and return to the average level (Figure 4I). The above results suggested that anlotinib could inhibit the proliferation of prostate cancer cells and induce apoptosis via the PI3K/AKT pathway.

Discussion

Medical treatment of metastatic prostate cancer heavily relies on androgen deprivation. However, most patients treated with anti-androgen often progress into a more aggressive androgen-independent and incurable type of prostate cancer. The activation of the AKT pathway plays a vital role in the progress of hormone-independent prostate cancer [20] and may promote drug resistance [21]. Studies have shown that activated AKT could mediate the phosphorylation status of proteins, including tuberous sclerosis complex 2, glycogen synthase kinase 3, forkhead box O transcription factor, p27, Bcl-2 antagonist of cell death, and endothelial nitric oxide synthase, which regulate a variety of biological processes such as coordination of cell growth and survival, proliferation, metabolism, and angiogenesis. The angiostatic effects of anlotinib have been demonstrated to be useful in the treatment of prostate cancer [22]. In addition, AKT mediates the phosphorylation and activation of the serine/threonine kinase mTOR complex, which is involved in protein translation and synthesis, angiogenesis, and cell cycle regulation [13, 21]. And the inhibitors of phosphorylation of these target proteins play a vital role in the development of prostate cancer [23]. Therefore, the development of AKT pathway-associated inhibitors may provide a novel approach to the treatment of prostate cancer [20].

Anlotinib is a tyrosine kinase inhibitor, independently developed in China, and is currently used in clinical practice for lung cancer and soft tissue sarcoma [15, 24]. Emerging evidence has suggested that the main targets of anlotinib are VEGFR, PDGFR, fibroblast growth factor receptor (FGFR), stem cell factor receptor (c-KIT), and other kinases [25]. The results of this study revealed that anlotinib exerted an inhibitory effect on the prostate cancer cell lines, DU145 and PC-3. The inhibitory effect of anlotinib was time- and dose-dependent. This finding was consistent with a previous report on lung cancer. The results also demonstrated that anlotinib affected prostate cancer cell cycle distribution, apoptosis, and invasion. Anlotinib significantly inhibited prostate cancer invasion and promoted the expression of apoptotic proteins. Therefore, we postulated that there could be other mechanisms underlying the effects of anlotinib. Immunoblotting results indicated that the phosphorylation of AKT protein and its downstream proteins was significantly attenuated following treatment of prostate cancer cells with anlotinib. This finding suggested that the effect of anlotinib could be closely associated with the inhibition of AKT phosphorylation. This observation was further confirmed by recovery experiments using the AKT pathway activator SC79. SC79 is the most commonly used AKT activator for inhibiting the AKT signaling pathway in recovery experiments [26–29]. The results showed that SC79 reversed the anti-proliferative effects of anlotinib. Furthermore, molecular docking analysis for the anlotinib-AKT1 interactions identified several potential interaction sites at multiple sites between anlotinib and AKT1, indicating that

anlotinib could act on the AKT pathway. AKT expression is associated with the prognosis of patients with prostate cancer, with increased AKT expression predicting poor prognosis [20]. In addition, AKT affects cell proliferation, apoptosis, and invasion in hormone-independent prostate cancer [20]. The above results partially explained the inhibitory effect of anlotinib on prostate cancer cell proliferation. Several toxic and side effects of anlotinib have been reported during its clinical application. Treatment of patients with advanced solid tumors may cause hand and foot skin reactions, high blood pressure, fatigue, and increased levels of lipases [30]. In some patients with NSCLC, administration of anlotinib led to obvious hypertriglyceridemia and hypercholesterolemia [31]. Therefore, in the clinical application of anlotinib in treating prostate cancer, the toxic and side effects should be thoroughly monitored to achieve the maximum treatment benefit. In the future, the inhibitory effect of anlotinib *in vivo* should be further explored using a tumor-bearing nude mouse model or based on a clinical phase I study. The results of this study are expected to promote the use of newly approved drugs and the investigation of their mechanisms of action, which in turn will lay the foundations for the development of similar drugs for the treatment of prostate cancer. Recent clinical studies have shown that anlotinib combined with immunotherapy can improve the therapeutic effect of lung cancer [32]. Therefore, the clinical benefits brought by the combination of immune checkpoint inhibitors and anlotinib may be assessed further. To reduce the side effects caused by anlotinib by decreasing the amount of anlotinib.

In summary, this study confirmed the role of anlotinib in inhibiting prostate cancer growth, cell invasion, and promoting apoptosis through the AKT pathway. These findings lay the foundation for the future clinical application of anlotinib in prostate cancer.

Supplementary information is available in the online version of the paper.

Acknowledgments: We thank the staff of the Department of Geriatrics of the Hwamei Hospital for all their efforts. This study was supported by the Ningbo Science and Technology Plan Project (grant no. 2018A10036).

References

- [1] WELCH HG, ALBERTSEN PC. Reconsidering Prostate Cancer Mortality – The Future of PSA Screening. *N Engl J Med* 2020; 382: 1557–1563. <https://doi.org/10.1056/NEJMms1914228>
- [2] CHEN R, ZHOU LQ, CAI XB, XIE LP, HUANG YR et al. Percent free prostate-specific antigen is effective to predict prostate biopsy outcome in Chinese men with prostate-specific antigen between 10.1 and 20.0 ng ml(-1). *Asian J Androl*. 2015; 17: 1017–1021. <https://doi.org/10.4103/1008-682X.150846>

- [3] HU JC, NGUYEN P, MAO J, HALPERN J, SHOAG J et al. Increase in Prostate Cancer Distant Metastases at Diagnosis in the United States. *JAMA Oncol* 2017; 3: 705–707. <https://doi.org/10.1001/jamaoncol.2016.5465>
- [4] NOGUCHI M, ARAI G, EGAWA S, OHYAMA C, NAITO S et al. Mixed 20-peptide cancer vaccine in combination with docetaxel and dexamethasone for castration-resistant prostate cancer: a randomized phase II trial. *Cancer Immunol Immunother* 2020; 69: 847–857. <https://doi.org/10.1007/s00262-020-02498-8>
- [5] LI K, FAN GR, CHEN CH, WANG ZP. [Methods for androgen receptor splice variant -7 detection: Advances in studies]. *Zhonghua Nan Ke Xue* 2019; 25: 1031–1035.
- [6] YUAN F, HANKEY W, WU D, WANG H, SOMARELLI J et al. Molecular determinants for enzalutamide-induced transcription in prostate cancer. *Nucleic Acids Res* 2019; 47: 10104–10114. <https://doi.org/10.1093/nar/gkz790>
- [7] HE L, FANG H, CHEN C, WU Y, WANG Y et al. Metastatic castration-resistant prostate cancer: Academic insights and perspectives through bibliometric analysis. *Medicine (Baltimore)* 2020; 99: e19760. <https://doi.org/10.1097/MD.00000000000019760>
- [8] MEHTÄLÄ J, ZONG J, VASSILEV Z, BROBERT G, GABARRÓ MS et al. Overall survival and second primary malignancies in men with metastatic prostate cancer. *PLoS One* 2020; 15: e0227552. <https://doi.org/10.1371/journal.pone.0227552>
- [9] CHEN X, QIAN H, QIAO H, DONG B, CHEN E et al. Tumor-Adhesive and pH-Degradable Microgels by Microfluidics and Photo-Cross-Linking for Efficient Antiangiogenesis and Enhanced Cancer Chemotherapy. *Biomacromolecules* 2020; 21: 1285–1294. <https://doi.org/10.1021/acs.biomac.0c00049>
- [10] TANG T, ABU-SBEIH H, MA W, LU Y, LUO W et al. Gastrointestinal Injury Related to Antiangiogenesis Cancer Therapy. *Clin Colorectal Cancer* 2020; 19: e117–e123. <https://doi.org/10.1016/j.clcc.2020.03.002>
- [11] XIE H, LAFKY JM, MORLAN BW, STELLA PJ, DAKHIL SR et al. Dual VEGF inhibition with sorafenib and bevacizumab as salvage therapy in metastatic colorectal cancer: results of the phase II North Central Cancer Treatment Group study N054C (Alliance). *Ther Adv Med Oncol* 2020; 12: 1758835920910913. <https://doi.org/10.1177/1758835920910913>
- [12] HONGO H, KOSAKA T, OYA M. Analysis of cabazitaxel-resistant mechanism in human castration-resistant prostate cancer. *Cancer Sci* 2018; 109: 2937–2945. <https://doi.org/10.1111/cas.13729>
- [13] DE BONO JS, DE GIORGI U, RODRIGUES DN, MAS-SARD C, BRACARDA S et al. Randomized Phase II Study Evaluating Akt Blockade with Ipatasertib, in Combination with Abiraterone, in Patients with Metastatic Prostate Cancer with and without PTEN Loss. *Clin Cancer Res* 2019; 25: 928–936. <https://doi.org/10.1158/1078-0432.CCR-18-0981>
- [14] QI P, CHEN M, ZHANG LX, SONG RX, HE ZH et al. A Meta-Analysis and Indirect Comparison of Endothelin A Receptor Antagonist for Castration-Resistant Prostate Cancer. *PLoS One* 2015; 10: e0133803. <https://doi.org/10.1371/journal.pone.0133803>
- [15] WANG G, SUN M, JIANG Y, ZHANG T, SUN W et al. Anlotinib, a novel small molecular tyrosine kinase inhibitor, suppresses growth and metastasis via dual blockade of VEGFR2 and MET in osteosarcoma. *Int J Cancer* 2019; 145: 979–993. <https://doi.org/10.1002/ijc.32180>
- [16] LIN B, SONG X, YANG D, BAI D, YAO Y et al. Anlotinib inhibits angiogenesis via suppressing the activation of VEGFR2, PDGFR β and FGFR1. *Gene* 2018; 654: 77–86. <https://doi.org/10.1016/j.gene.2018.02.026>
- [17] LU J, ZHONG H, WU J, CHU T, ZHANG L et al. Circulating DNA-Based Sequencing Guided Anlotinib Therapy in Non-Small Cell Lung Cancer. *Adv Sci (Weinh)* 2019; 6: 1900721. <https://doi.org/10.1002/advs.201900721>
- [18] TANG Y, OU Z, YAO Z, QIAO G. A case report of immune checkpoint inhibitor nivolumab combined with anti-angiogenesis agent anlotinib for advanced esophageal squamous cell carcinoma. *Medicine (Baltimore)* 2019; 98: e17164. <https://doi.org/10.1097/MD.00000000000017164>
- [19] HE X, HE C, SUN G, JIANG H, XIAO Y et al. Case of Treating Advanced Prostate, Bladder Double Primary Cancer with Anlotinib and Literature Review. *MedSBE* 2019; 238–242. <https://doi.org/10.25236/medsbe.2019.050>
- [20] CARIAGA-MARTINEZ AE, LÓPEZ-RUIZ P, NOMBELABLANCO MP, MOTIÑO O, GONZÁLEZ-CORPAS A et al. Distinct and specific roles of AKT1 and AKT2 in androgen-sensitive and androgen-independent prostate cancer cells. *Cell Signal* 2013; 25: 1586–1597. <https://doi.org/10.1016/j.cellsig.2013.03.019>
- [21] BRAGLIA L, ZAVATTI M, VINCETI M, MARTELLI AM, MARMIROLI S. Deregulated PTEN/PI3K/AKT/mTOR signaling in prostate cancer: Still a potential druggable target. *Biochim Biophys Acta Mol Cell Res* 2020; 118731. <https://doi.org/10.1016/j.bbamcr.2020.118731>
- [22] Liang L, Hui K, Hu C, Wen Y, Yang S et al. Autophagy inhibition potentiates the anti-angiogenic property of multikinase inhibitor anlotinib through JAK2/STAT3/VEGFA signaling in non-small cell lung cancer cells. *J Exp Clin Cancer Res* 2019; 38: 71. <https://doi.org/10.1186/s13046-019-1093-3>
- [23] GAO Y, GARTENHAUS RB, LAPIDUS RG, HUSSAIN A, ZHANG Y et al. Differential IKK/NF- κ B Activity Is Mediated by TSC2 through mTORC1 in PTEN-Null Prostate Cancer and Tuberous Sclerosis Complex Tumor Cells. *Mol Cancer Res* 2015; 13: 1602–1614. <https://doi.org/10.1158/1541-7786.MCR-15-0213>
- [24] CHEN D, XU J, ZHAO Y, CHU T, ZHANG H et al. Prognostic value of tumor cavitation in extensive-stage small-cell lung cancer patients treated with anlotinib. *J Cancer Res Clin Oncol* 2020; 146: 401–406.
- [25] SHEN G, ZHENG F, REN D, DU F, DONG Q et al. Anlotinib: a novel multi-targeting tyrosine kinase inhibitor in clinical development. *J Hematol Oncol* 2018; 11: 120. <https://doi.org/10.1186/s13045-018-0664-7>
- [26] SUN H, HUANG M, YAO N, HU Y, LI Y et al. The cycloartane triterpenoid ADCX impairs autophagic degradation through Akt overactivation and promotes apoptotic cell death in multidrug-resistant HepG2/ADM cells. *Biochem Pharmacol* 2017; 146: 87–100. <https://doi.org/10.1016/j.bcp.2017.10.012>

- [27] WU L, WANG W, DAI M, LI H, CHEN C et al. PPAR α ligand, AVE8134, and cyclooxygenase inhibitor therapy synergistically suppress lung cancer growth and metastasis. *BMC Cancer* 2019; 19: 1166. <https://doi.org/10.1186/s12885-019-6379-5>
- [28] ZHANG D, WAY JS, ZHANG X, MARENINOV S, BERGSNEIDER M et al. Effect of Everolimus in Treatment of Aggressive Prolactin-Secreting Pituitary Adenomas. *J Clin Endocrinol Metab* 2019; 104: 1929–1936. <https://doi.org/10.1210/jc.2018-02461>
- [29] CÁRDENAS S, COLOMBERO C, PANELO L, DAKARAPU R, FALCK JR et al. GPR75 receptor mediates 20-HETE-signaling and metastatic features of androgen-insensitive prostate cancer cells. *Biochim Biophys Acta Mol Cell Biol Lipids* 2020; 1865: 158573. <https://doi.org/10.1016/j.bbalip.2019.158573>
- [30] SUN Y, NIU W, DU F, DU C, LI S et al. Safety, pharmacokinetics, and antitumor properties of anlotinib, an oral multi-target tyrosine kinase inhibitor, in patients with advanced refractory solid tumors. *J Hematol Oncol* 2016; 9: 105. <https://doi.org/10.1186/s13045-016-0332-8>
- [31] SI X, ZHANG L, WANG H, ZHANG X, WANG M et al. Management of anlotinib-related adverse events in patients with advanced non-small cell lung cancer: Experiences in ALTER-0303. *Thorac Cancer* 2019; 10: 551–556. <https://doi.org/10.1111/1759-7714.12977>
- [32] YANG S, ZHANG W, CHEN Q, GUO Q. Clinical Investigation of the Efficacy and Safety of Anlotinib with Immunotherapy in Advanced Non-Small Cell Lung Cancer as Third-Line Therapy: A Retrospective Study. *Cancer Manag Res* 2020; 12: 10333–10340. <https://doi.org/10.2147/CMAR.S280096>